Supporting Information

Aromatic Stabilization of Functionalized Corannulene Cations

Jingbai Li, Andrey Yu. Rogachev*

Department of Chemistry, Illinois Institute of Technology, Chicago, IL 60616, USA

To whom correspondence should be addressed:
E-mail: andrey.rogachev@gmail.com and/or andrey.rogachev@iit.edu (A.Yu. Rogachev)

Figure S1. Equilibrium geometry configurations for all systems considered in this study along with labeling scheme. S3

Figure S2. ACID isosurfaces of neutral corannulene. Current density vectors are plotted onto the ACID isosurface to indicate dia- and paratropic ring currents. Green arrow in the ball-and-stick models shows applied magnetic field direction. S3

Figure S3. π-Contribution to the ACID isosurface of neutral corannulene. Current density vectors are plotted onto the ACID isosurface to indicate dia- and paratropic ring currents. Green arrow in the ball-and-stick models shows applied magnetic field direction S4

Figure S4. ACID isosurfaces of cationic $[CH_3\text{-}hub\text{-}C_{20}H_{10}]^+$. Current density vectors are plotted onto the ACID isosurface to indicate dia- and paratropic ring currents. Green arrow in the ball-and-stick models shows applied magnetic field direction. S4

Figure S5. π-Contribution to the ACID isosurface of cationic $\{CH_3\text{-}hub\text{-}C_{20}H_{10}]^+$. Current density vectors are plotted onto the ACID isosurface to indicate dia- and paratropic ring currents. Green arrow in the ball-and-stick models shows applied magnetic field direction.S5

Figure S6. ACID isosurfaces of cationic $[CH_3\text{-}rim\text{-}C_{20}H_{10}]^+$. Current density vectors are plotted onto the ACID isosurface to indicate dia- and paratropic ring currents. Green arrow in the ball-and-stick models shows applied magnetic field direction. S5

Figure S7. π-Contribution to the ACID isosurface of cationic $\{CH_3\text{-}rim\text{-}C_{20}H_{10}]^+$. Current density vectors are plotted onto the ACID isosurface to indicate dia- and paratropic ring currents. Green arrow in the ball-and-stick model shows applied magnetic field direction. S6

Figure S8. ACID isosurfaces of cationic $[CH_3\text{-}spoke\text{-}C_{20}H_{10}]^+$. Current density vectors are plotted onto the ACID isosurface to indicate dia- and paratropic ring currents. Green arrow in the ball-and-stick models shows applied magnetic field direction. S6
Figure S8. π-Contribution to the ACID isosurface of cationic $\{CH_3\text{-}spoke\text{-}C_{20}H_{10}]^+$. Current density vectors are plotted onto the ACID isosurface to indicate dia- and paratropic ring currents. Green arrow in the ball-and-stick model shows applied magnetic field direction S7
Table S1. Cartesian coordinates for neutral corannulene, $C_{20}H_{10}$, optimized at the PBE0/cc-pVTZ level of theory S7
Table S2. Cartesian coordinates for $[CH_3\text{-}hub\text{-}C_{20}H_{10}]^+$, optimized at the PBE0/cc-pVTZ level of theory S8
Table S3. Cartesian coordinates for $[CH_3\text{-}rim\text{-}C_{20}H_{10}]^+$, optimized at the PBE0/cc-pVTZ level of theory S8
Table S4. Cartesian coordinates for $[CH_3\text{-}spoke\text{-}C_{20}H_{10}]^+$, optimized at the PBE0/cc-pVTZ level of theory S9
Table S5. Cartesian coordinates for benzene, C_6H_6, optimized at the PBE0/cc-pVTZ level of theory S9
Table S6. Cartesian coordinates for cyclopentadiene, C_5H_6, optimized at the PBE0/cc-pVTZ level of theory S10
Table S7. Cartesian coordinates for cyclopentadienyl-anionm $C_5H_5^-$, optimized at the PBE0/cc-pVTZ level of theory S10
Table S8. Absolute energies for all systems considered (PBE0/cc-pVTZ) S10

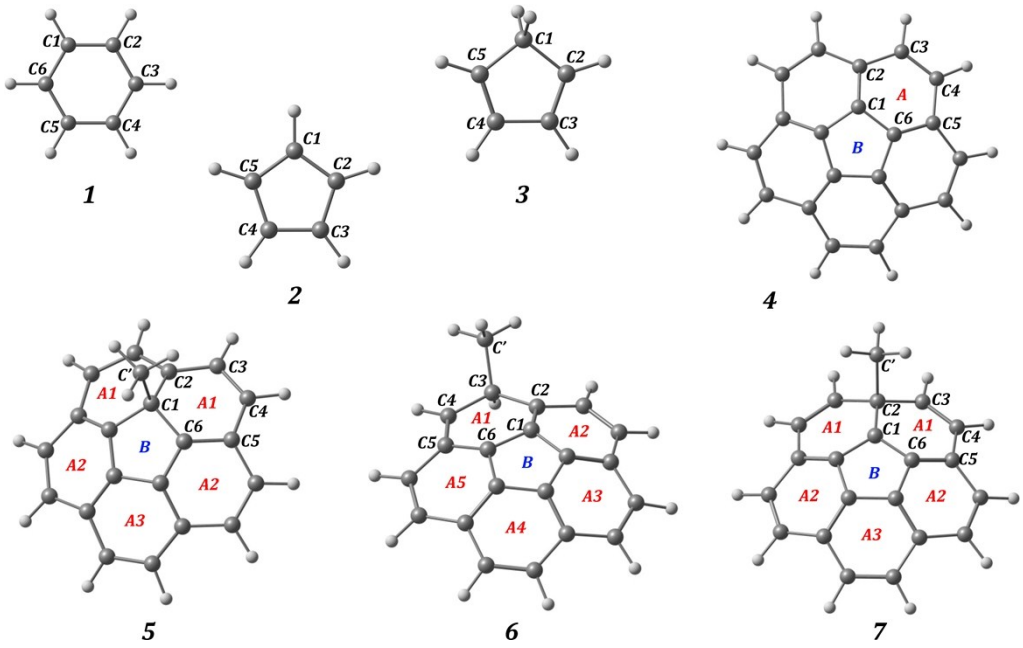

Figure S1. Equilibrium geometry configurations for all systems considered in this study along with labeling scheme.

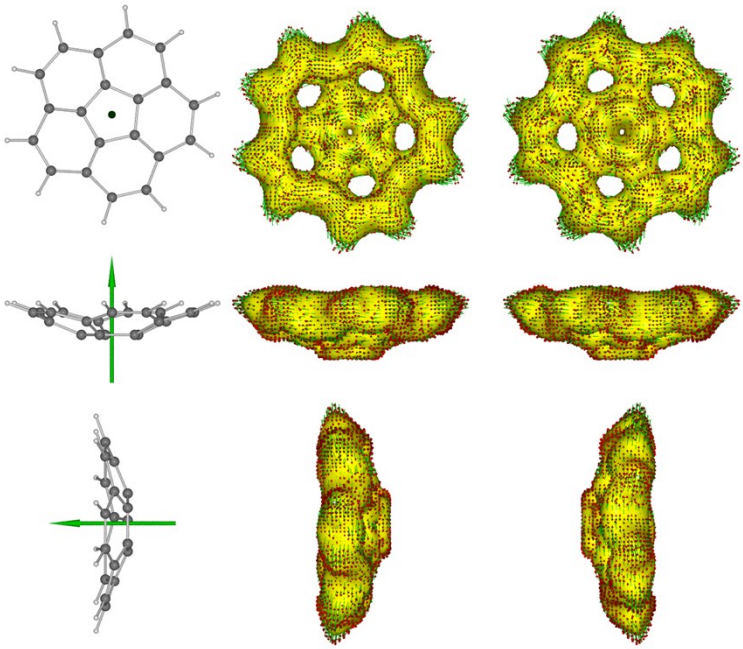

Figure S2. ACID isosurfaces of neutral corannulene. Current density vectors are plotted onto the ACID isosurface to indicate dia- and paratropic ring currents. Green arrow in the ball-and-stick models shows applied magnetic field direction.

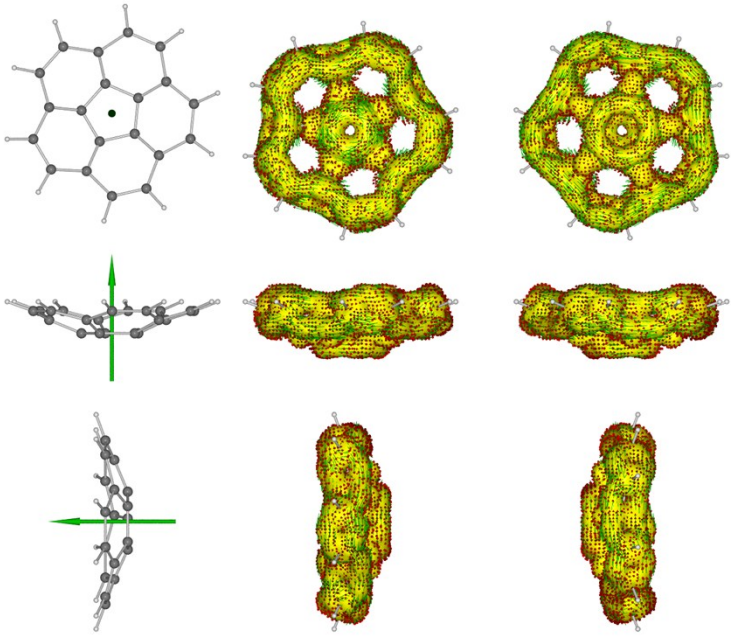

Figure S3. π-Contribution to the ACID isosurface of neutral corannulene. Current density vectors are plotted onto the ACID isosurface to indicate dia- and paratropic ring currents. Green arrow in the ball-and-stick models shows applied magnetic field direction.

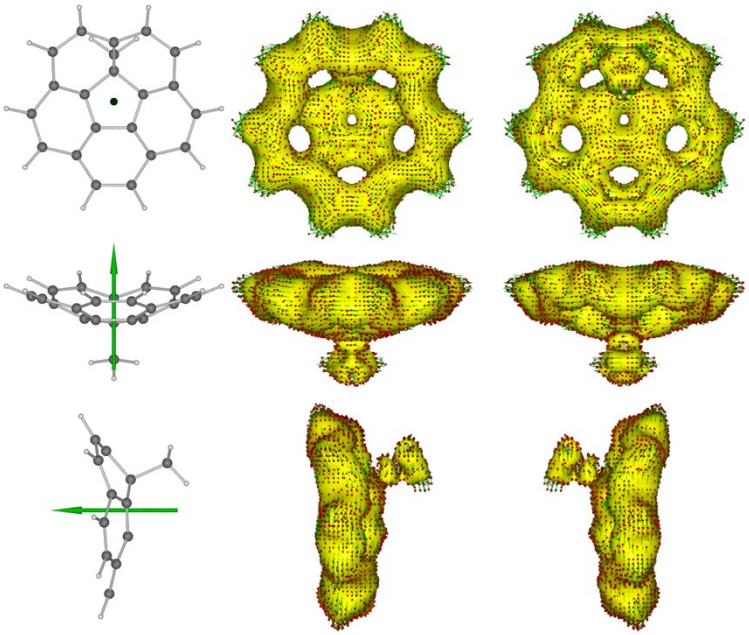

Figure S4. ACID isosurfaces of cationic $[CH_3\text{-}hub\text{-}C_{20}H_{10}]^+$. Current density vectors are plotted onto the ACID isosurface to indicate dia- and paratropic ring currents. Green arrow in the ball-and-stick models shows applied magnetic field direction.

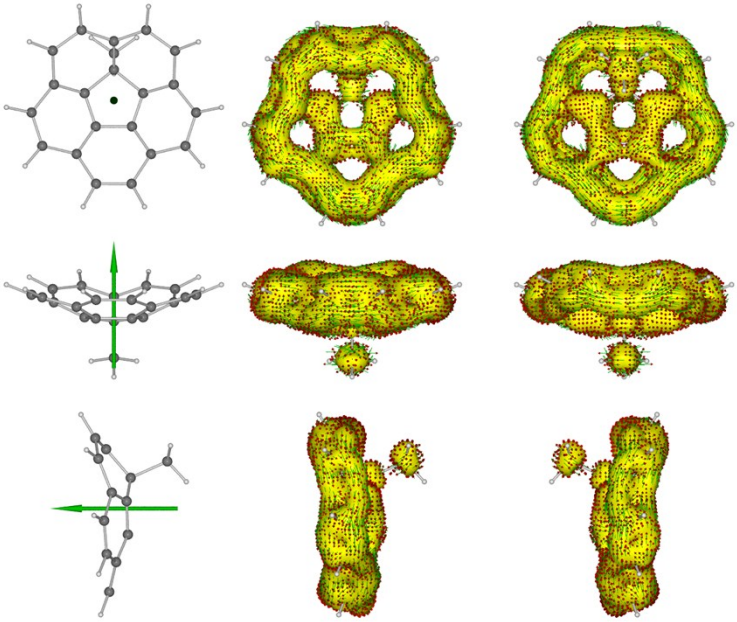

Figure S5. π-Contribution to the ACID isosurface of cationic $\{CH_3\text{-}hub\text{-}C_{20}H_{10}]^+$. Current density vectors are plotted onto the ACID isosurface to indicate dia- and paratropic ring currents. Green arrow in the ball-and-stick models shows applied magnetic field direction.

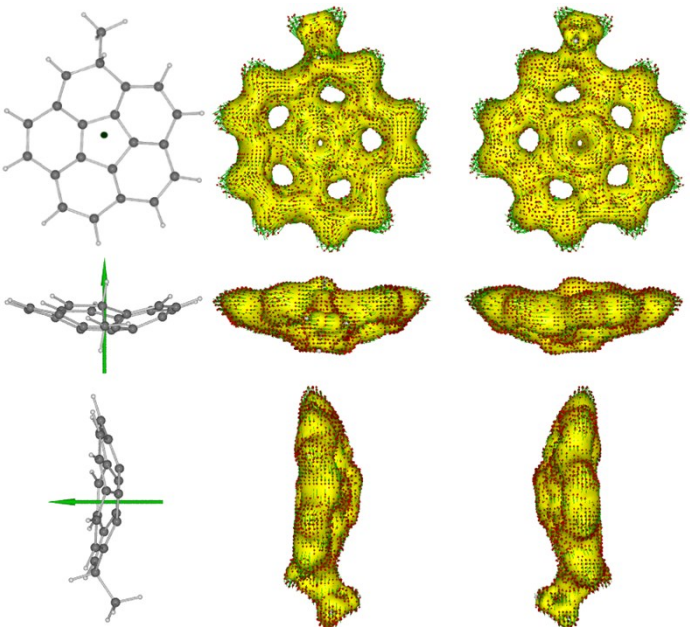

Figure S6. ACID isosurfaces of cationic $[CH_3\text{-}rim\text{-}C_{20}H_{10}]^+$. Current density vectors are plotted onto the ACID isosurface to indicate dia- and paratropic ring currents. Green arrow in the ball-and-stick models shows applied magnetic field direction.

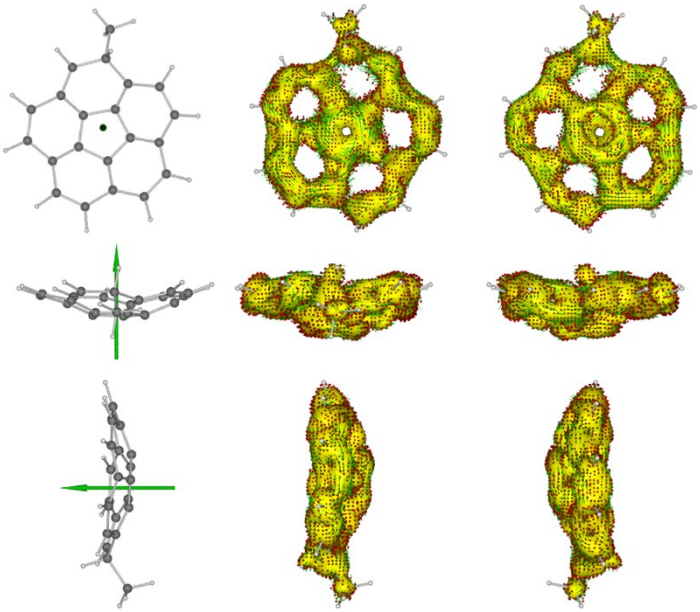

Figure S7. π-Contribution to the ACID isosurface of cationic $\{CH_3\text{-}rim\text{-}C_{20}H_{10}]^+$. Current density vectors are plotted onto the ACID isosurface to indicate dia- and paratropic ring currents. Green arrow in the ball-and-stick model shows applied magnetic field direction.

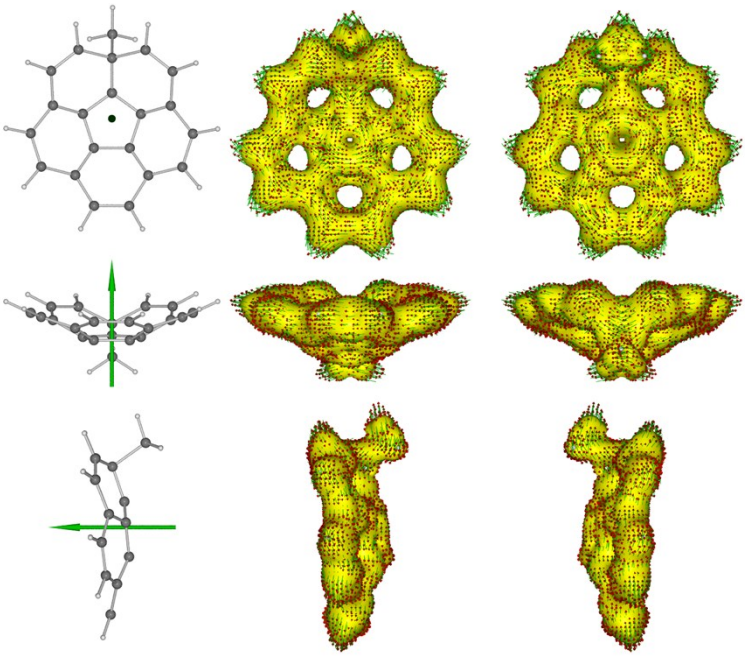

Figure S8. ACID isosurfaces of cationic $[CH_3\text{-}spoke\text{-}C_{20}H_{10}]^+$. Current density vectors are plotted onto the ACID isosurface to indicate dia- and paratropic ring currents. Green arrow in the ball-and-stick models shows applied magnetic field direction.

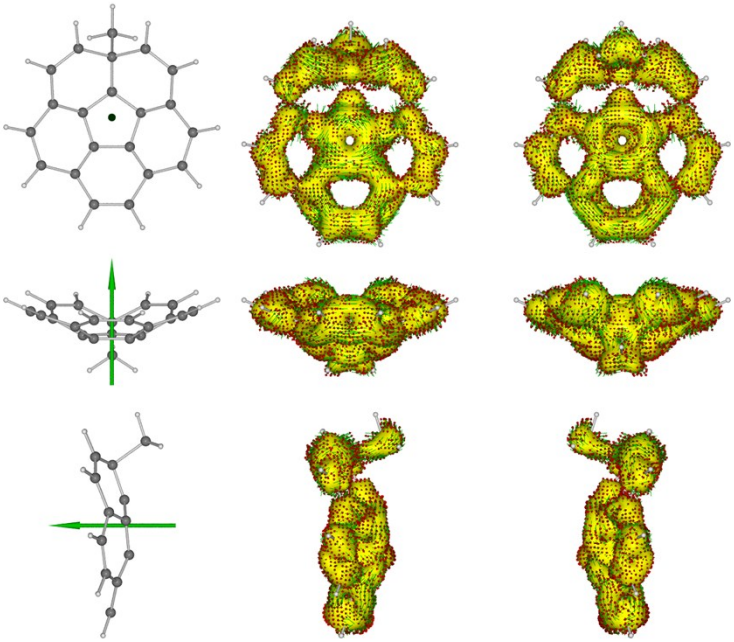

Figure S9. π-Contribution to the ACID isosurface of cationic $\{CH_3\text{-}spoke\text{-}C_{20}H_{10}\}^+$. Current density vectors are plotted onto the ACID isosurface to indicate dia- and paratropic ring currents. Green arrow in the ball-and-stick model shows applied magnetic field direction.

Table S1. Cartesian coordinates for neutral corannulene, $C_{20}H_{10}$, optimized at the PBE0/cc-pVTZ level of theory.

C	0.635178031	3.098269931	-6.998384289
C	1.229834001	4.329144098	-7.152379591
C	1.636139247	4.949901677	-5.920206073
C	1.614050766	4.272758827	-4.718469711
C	1.183307649	2.903802546	-4.622599812
C	0.612494046	2.406912494	-5.771292447
C	0.527623107	1.028714956	-6.049581577
C	1.008165419	0.062606497	-5.196386956
C	1.407186666	0.556333686	-3.905680079
C	1.490515443	1.906117886	-3.633177375
H	2.059577789	5.948408434	-5.939917997
H	2.021016296	4.766591648	-3.842555964
H	1.887154236	2.212990813	-2.671282317
H	1.741733309	-0.142944771	-3.146849991
C	1.353720774	1.171432894	-10.039570983
C	1.289213628	-0.081199984	-9.465148301
C	1.083219089	2.368629022	-9.289715008
H	1.595362704	-0.935680990	-10.059189742
C	0.947144087	-0.268025424	-8.080624984
C	0.564225676	2.147267456	-8.035090571
C	0.498138923	0.868295421	-7.448736815
H	1.708085840	1.250629968	-11.061761519
C	1.580226710	4.653117933	-8.509195093
C	1.510434759	3.721792832	-9.524601711
C	1.276758985	-1.203209869	-5.824186032
C	1.247823533	-1.360250599	-7.194490233
H	1.998990056	5.628255618	-8.733851593
H	1.876978215	4.002912573	-10.506090032
H	1.601545313	-2.041542292	-5.217191716

H	1.551024128	-2.315737396	-7.609039120

Table S2. Cartesian coordinates for $[CH_3\text{-}hub\text{-}C_{20}H_{10}]^+$, optimized at the PBE0/cc-pVTZ level of theory.

C	-1.921459206	2.696202805	0.276885524
C	1.828768556	2.511586296	0.618196754
C	2.852714761	-1.100382439	0.753732430
C	-0.258877388	-3.247663625	0.399965160
C	-3.196010675	-0.888692256	0.181525046
H	-2.751417240	3.321371744	0.583731710
H	2.118998107	3.447535369	1.084844182
H	3.777732829	-1.134236764	1.317774861
H	0.000514454	-4.220586590	0.800386461
H	-4.064678936	-1.445854313	0.513886991
C	0.507985606	2.382028363	0.090034769
C	2.344274855	0.138234816	0.324054671
C	0.786547372	-2.307924650	0.103455276
C	-1.983423380	-1.582775961	-0.083787558
C	-2.156816994	1.332746547	-0.091517525
C	0.242836093	1.161971148	-0.491573173
C	1.231190028	0.069872810	-0.644371079
C	0.379236849	-1.131200470	-0.485170889
C	-0.948886474	-0.770634223	-0.539944347
C	-1.033261259	0.646476855	-0.543561518
C	-0.641606168	3.193179983	0.381412039
C	2.702115190	1.430702317	0.747165385
C	2.113469426	-2.277733191	0.631223410
C	-1.588418936	-2.906443770	0.292580533
C	-3.278758107	0.501200614	0.177975614
H	-0.499175021	4.192171745	0.776081447
H	3.616134570	1.576803636	1.311072588
H	2.512286566	-3.170216284	1.102673583
H	-2.338533663	-3.623737535	0.603530172
H	-4.207336883	0.953073900	0.508177034
C	1.877025801	0.104706098	-2.075431126
H	2.441328262	1.027802174	-2.200859639
H	2.543952490	-0.747610096	-2.197749437
H	1.085158013	0.057822796	-2.821603650

Table S3. Cartesian coordinates for $[CH_3\text{-}rim\text{-}C_{20}H_{10}]^+$, optimized at the PBE0/cc-pVTZ level of theory.

C	-1.994699557	2.716029083	0.398066954
C	1.802748319	2.553330864	0.487867918
C	2.907070133	-1.150043456	0.424446494
C	-0.393943733	-3.279536413	0.321566519
C	-3.322645461	-0.866693265	0.310016320
H	-2.805047260	3.341041652	0.754563875
H	2.150465235	3.503554206	0.877514206
H	3.300430648	-1.108060141	1.453038803
H	-0.134884151	-4.286790893	0.624253981
H	-4.185502630	-1.431242835	0.642542582
C	0.427837816	2.411909205	0.092076102
C	2.264082400	0.175155692	0.114645022
C	0.666711190	-2.319159471	0.060361389
C	-2.110667638	-1.548718526	-0.017206527
C	-2.261604738	1.355751125	0.017427830
C	0.126178662	1.191874148	-0.464806750
C	1.017574172	0.105996340	-0.434884742
C	0.236986652	-1.076949983	-0.431625879
C	-1.109894072	-0.728816402	-0.507848255
C	-1.186205481	0.677873003	-0.500371903
C	-0.711601886	3.220365724	0.431731614
C	2.680877478	1.482912992	0.500747405
C	1.992385833	-2.341750680	0.429720907
C	-1.708430139	-2.905511609	0.290636899

C	-3.391441174	0.515661367	0.326387585
H	-0.560556018	4.223097222	0.814145677
H	3.676089424	1.641194272	0.900140436
H	2.439670153	-3.257214420	0.809441293
H	-2.462612133	-3.627196331	0.581208991
H	-4.312388525	0.973057806	0.671521059
C	4.140286282	-1.445235988	-0.471920795
H	4.861960541	-0.636114944	-0.372136420
H	4.620589895	-2.375823467	-0.171186155
H	3.840469759	-1.520775874	-1.516372441

Table S4. Cartesian coordinates for $[CH_3\text{-}spoke\text{-}C_{20}H_{10}]^+$, optimized at the PBE0/cc-pVTZ level of theory.

C	-1.945026788	2.668259491	0.336209073
C	1.814090086	2.458426512	0.783185137
C	2.829132730	-1.192225701	0.759097354
C	-0.352805436	-3.209803941	0.488597207
C	-3.301773186	-0.856345726	0.132274573
H	-2.773741864	3.296914966	0.643215287
H	2.091645029	3.384507685	1.273127617
H	3.824950357	-1.247125842	1.185433047
H	-0.119536285	-4.172110883	0.928163016
H	-4.179661643	-1.420840523	0.423595743
C	0.476231123	2.325760944	0.236455013
C	2.448601127	0.110665322	0.098678915
C	0.701268245	-2.286063165	0.214546050
C	-2.067923992	-1.541031365	-0.113926091
C	-2.207394306	1.322845714	-0.107964925
C	0.211246085	1.144609351	-0.432033153
C	1.084173420	0.046885299	-0.376362628
C	0.321184679	-1.128846166	-0.440425033
C	-1.034981057	-0.760512694	-0.577160813
C	-1.103238550	0.648582200	-0.573480471
C	-0.662434682	3.142437665	0.514035706
C	2.695831800	1.433683492	0.783094729
C	2.049938278	-2.297081265	0.750397545
C	-1.675583445	-2.857910406	0.320098711
C	-3.369176131	0.520714175	0.133988149
H	-0.523784561	4.117763285	0.964577755
H	3.678629002	1.577519339	1.218596534
H	2.419319119	-3.199118071	1.224402153
H	-2.438682348	-3.565347161	0.625792227
H	-4.298049011	0.996685607	0.425559657
C	3.386490436	0.172584879	-1.196506460
H	3.138506821	1.055688275	-1.781756656
H	4.422632638	0.230104956	-0.867806951
H	3.240422308	-0.725616249	-1.792838022

Table S5. Cartesian coordinates for benzene, C_6H_6, optimized at the PBE0/cc-pVTZ level of theory.

C	2.595240480	4.708081613	-10.945974139
C	1.446383198	4.355573059	-10.252133399
C	3.744097762	5.060590168	-10.252133399
H	0.549213856	4.080362834	-10.793968827
H	4.641267105	5.335800392	-10.793968827
C	1.446383197	4.355573058	-8.864521054
C	3.744097763	5.060590168	-8.864521054
H	0.549213856	4.080362834	-8.322685626
H	4.641267105	5.335800392	-8.322685626
C	2.595240480	4.708081613	-8.170680312
H	2.595240480	4.708081613	-7.087069066
H	2.595240480	4.708081613	-12.029585387

Table S6. Cartesian coordinates for cyclopentadiene, C_5H_6, optimized at the PBE0/cc-pVTZ level of theory.

C	-0.028070194	0.026503591	-1.207855054
C	0.025240452	1.135472374	-0.454060532
C	0.067657525	0.744743834	0.986392323
C	0.031292660	-0.747012324	0.941696227
C	-0.023801432	-1.146299095	-0.338237600
H	-0.068155451	-0.009643464	-2.288363046
H	0.036634896	2.157426849	-0.805283872
H	0.047537033	-1.379957354	1.817475928
H	-0.059312623	-2.169898597	-0.686647220
H	-0.778483984	1.159681867	1.548609596
H	0.969753824	1.118395553	1.487226014

Table S7. Cartesian coordinates for cyclopentadienyl-anionm $C_5H_5^-$, optimized at the PBE0/cc-pVTZ level of theory.

C	-0.008627699	-0.011213611	-1.213440480
C	-0.008627699	1.134790065	-0.397094849
C	-0.008627699	0.712516539	0.945113083
C	-0.008627699	-0.694347692	0.958341502
C	-0.008627699	-1.141690882	-0.375698779
H	-0.008627699	-0.021396447	-2.298978570
H	-0.008627699	2.163998880	-0.742270214
H	-0.008627699	-1.324209119	1.842476647
H	-0.008627699	-2.177280955	-0.701459863
H	-0.008627699	1.358833221	1.817399373

Table S8. Absolute energies for all systems considered (PBE0/cc-pVTZ).

Compound	Energy, a.u.
$C_{20}H_{10}$	-767.4902595322
$[CH_3\text{-}\textit{hub}\text{-}C_{20}H_{10}]^+$	-807.1063665731
$[CH_3\text{-}\textit{rim}\text{-}C_{20}H_{10}]^+$	-807.1026843586
$[CH_3\text{-}\textit{spoke}\text{-}C_{20}H_{10}]^+$	-807.0814173521
C_6H_6	-232.0406581856
C_5H_6	-193.9293785508
$C_5H_5^-$	-193.3482088665